FEMS Microbiology Ecology, 94, 2018, fix177

doi: 10.1093/femsec/fix177
Advance Access Publication Date: 5 December 2017
Research Article

RESEARCH ARTICLE

Quantitative analysis of O_2 and Fe^{2+} profiles in gradient tubes for cultivation of microaerophilic Iron(II)-oxidizing bacteria

U. Lueder[1], G. Druschel[2], D. Emerson[3], A. Kappler[1,4] and C. Schmidt[1,*]

[1]Geomicrobiology Group, Center for Applied Geoscience (ZAG), University of Tuebingen, Sigwartstrasse 10, D-72076 Tuebingen, Germany, [2]Department of Earth Sciences, Indiana University-Purdue University, 723 W Michigan Street, SL118, Indianapolis, IN 46202, USA, [3]Bigelow Laboratory for Ocean Sciences, 60 Bigelow Drive, East Boothbay, ME 04544, USA and [4]Center for Geomicrobiology, Department of Bioscience, Aarhus University, Ny Munkegade 114, Building 1540, 8000 Aarhus, Denmark

*Corresponding authors: Geomicrobiology, Center for Applied Geosciences, University of Tuebingen, Sigwartstrasse 10, D-72076 Tuebingen, Germany. Tel: +49-7071-2975496; Fax: +49-7071-29-295059; E-mail: caroline.schmidt@uni-tuebingen.de

One sentence summary: The work provides insights on optimal growth conditions of microaerophilic iron(II)-oxidizing bacteria under which they can compete with fast chemical iron(II) oxidation by oxygen.

Editor: Tillmann Lueders

ABSTRACT

The classical approach for the cultivation of neutrophilic microaerophilic Fe(II)-oxidizing bacteria is agar-based gradient tubes where these bacteria find optimal growth conditions in opposing gradients of oxygen (O_2) and dissolved Fe(II) (Fe^{2+}). The goals of this study were to quantify the temporal development of O_2 and Fe^{2+} concentrations over time, to compare abiotic and microbially inoculated tubes and to test the suitability of different Fe(II)-sources for the cultivation of freshwater and marine microaerophilic Fe(II)-oxidizers. O_2 and Fe^{2+} gradients were monitored on a high spatial resolution as a function of time applying amperometric and voltammetric microsensors. Fe(II)-oxidizers could be cultivated well with FeS and zero-valent iron powder as Fe(II)-source, but $FeCO_3$ and $FeCl_2$ are extremely sensitive for this application. Fe(III) minerals accumulated in inoculated tubes within the first days in regions with an O_2 concentration of 20–40 μM and were confirmed to be related to bacterial growth. Microbial Fe(II) oxidation could compete only for the first days with the abiotic reaction after which heterogeneous Fe(II) oxidation, catalyzed by Fe(III) minerals, dominated. Our results imply that transfer of cultures to fresh tubes within 48–72 h is crucial to provide optimal growth conditions for microaerophilic Fe(II)-oxidizers, particularly for the isolation of new strains.

Keywords: microaerophilic iron(II) oxidation; iron(II)-oxidizing bacteria; iron cycling; gradient tubes

INTRODUCTION

Iron is one of the most dominant chemical elements in the continental crust (Taylor 1964), and it is an important component of several geological, mineralogical, environmental and microbial processes. As an essential micronutrient, iron is integrated in many cellular compounds and has high relevance in modern and ancient, as well as in extraterrestrial environments. In the environment, iron is often involved in biotic and abiotic redox processes (Melton *et al.* 2014) and mainly occurs in two redox states: as oxidized ferric iron (Fe(III)) or as reduced ferrous iron (Fe(II)). At circumneutral pH, Fe(III) is poorly soluble (Cornell and Schwertmann 2003) and normally occurs as solid Fe(III)

Received: 14 September 2017; **Accepted:** 4 December 2017

minerals; soluble Fe(III) (Fe^{3+}), either, freely dissolved, or more often complexed with organic molecules, is only present at very low concentration in the range of 10^{-6}–10^{-9} M (Taillefert Bono and Luther 2000; Kappler and Straub 2005). In contrast, Fe(II) is more soluble and therefore more bioavailable for organisms (Melton *et al.* 2014); however, at neutral pH, it is rapidly chemically oxidized in the presence of oxygen (O_2) (Davison and Seed 1983; Stumm and Morgan 1996). During homogenous abiotic Fe(II) oxidation, dissolved Fe(II) (Fe^{2+}) is oxidized by dissolved O_2 and other intermediate oxygen species that are formed during the stepwise reduction of O_2 (Melton *et al.* 2014). The formed Fe^{3+} will instantaneously react with water and precipitate as the Fe(III) oxyhydroxide mineral with a rusty-orange color (Emerson and Weiss 2004). These mineral precipitates serve as catalyst for further chemical Fe(II) oxidation, an autocatalysis reaction also called heterogeneous Fe(II) oxidation (Tamura Goto and Nagayama 1976; Rentz *et al.* 2007). Both, heterogeneous and homogeneous Fe(II) oxidation run in parallel; however, heterogeneous Fe(II) oxidation is faster so that homogeneous Fe(II) oxidation becomes of minor importance (Stumm and Sulzberger 1992; Park and Dempsey 2005) once sufficient iron oxyhydroxides are formed. Besides the chemical redox transformations, microbes contribute to a large extent to the cycling between the redox states of iron (Weber Achenbach and Coates 2006; Konhauser Kappler and Roden 2011). Fe(III)-reducing bacteria can reduce Fe(III) to Fe(II) under anoxic conditions using electron donors such as hydrogen (H_2), acetate or lactate (Kashefi and Lovley 2000; Lovley *et al.* 2011). On the other hand, Fe(II) can be oxidized enzymatically by photoautotrophic Fe(II)-oxidizers using light energy with bicarbonate as electron acceptor and carbon source (Widdel *et al.* 1993; Hegler *et al.* 2008). Other microorganisms couple Fe(II) oxidation to nitrate (NO_3^-) reduction under anoxic conditions (Straub *et al.* 1996). However, most nitrate-reducing Fe(II)-oxidizers need an additional organic cosubstrate to continually oxidize Fe(II) to Fe(III) (Straub *et al.* 1996; Klueglein *et al.* 2014). Microaerophilic Fe(II)-oxidizers can oxidize Fe(II) as a sole electron donor using O_2 as electron acceptor for lithotrophic growth (Emerson and Moyer 1997). Bacteria that are capable of aerobic neutrophilic Fe(II) oxidation have to compete with the abiotic reaction due to the short half-life of Fe^{2+} in oxygenated water (Singer and Stumm 1970; Stumm and Morgan 1996; Hegler *et al.* 2012). Under microoxic conditions, the half-life of Fe(II) can be more than 300 times longer (Roden *et al.* 2004). It was shown that abiotic Fe(II) oxidation dominated at O_2 concentrations of 275 μM, while at 50 μM and below, microbial Fe(II) oxidation was faster than the abiotic reaction (Druschel *et al.* 2008). As a result neutrophilic Fe(II)-oxidizers are often restricted to live in areas with a constant source of Fe(II) and low O_2 concentrations where the biotic oxidation rates can outcompete the abiotic rates (Emerson and Weiss 2004).

The demands of microaerophilic Fe(II)-oxidizers in combination with the kinetics of abiotic Fe(II) oxidation make cultivation in laboratory setups difficult. The traditional technique used is the cultivation of microaerophilic Fe(II)-oxidizers in agar-stabilized gradient tubes with opposing gradients of Fe^{2+} and O_2 (Emerson and Moyer 1997; Sobolev and Roden 2001; Emerson and Moyer 2002; Neubauer Emerson and Megonigal 2002; Edwards *et al.* 2003; Weiss *et al.* 2003; Emerson and Floyd 2005; Weiss *et al.* 2007; Druschel *et al.* 2008; Swanner Nell and Templeton 2011; Lin *et al.* 2012; MacDonald *et al.* 2014; Laufer *et al.* 2016). By analyzing Fe^{2+} and O_2 concentrations at high spatial resolution as well as the development of the competitive pressure between biotic and abiotic Fe(II) oxidation, conclusions about optimal substrate demands and habitat limitations by kinetic constraints can be drawn. So far, the geochemical conditions in gradient tubes were examined only in a few studies (Druschel *et al.* 2008; Swanner Nell and Templeton 2011). However, spatially highly resolved measurements as a function of time are missing. These measurements are important to determine the optimal time point for transfer of cultures, which is a critical parameter for isolation and continuous cultivation. Also, different Fe(II)-sources (Emerson and Moyer 1997; Druschel *et al.* 2008; Swanner Nell and Templeton 2011; Emerson *et al.* 2013; MacDonald *et al.* 2014) for gradient tubes are mentioned in the literature, but they have not been compared systematically in terms of suitability for growth of microaerophilic Fe(II)-oxidizers.

Therefore, the goals of this study were (i) to test and compare iron sulfide (FeS), iron carbonate ($FeCO_3$), zero-valent iron powder (ZVI) and iron chloride ($FeCl_2$) as Fe(II)-sources for the suitability of growth of selected freshwater and marine neutrophilic microaerophilic Fe(II)-oxidizing bacteria, (ii) to quantify O_2 and Fe^{2+} profiles as a function of time at high spatial resolution using amperometric and voltammetric microsensors and (iii) to identify exact physico-chemical conditions for optimal growth to give recommendations and improve isolation and cultivation of new microaerophilic Fe(II)-oxidizers.

MATERIAL AND METHODS

Cultivation of bacteria

Gradient tube preparation was based on Emerson and Floyd (2005). Opposing gradients of Fe^{2+} and O_2 in screw-cap vials (8 ml, 61 × 16.6 mm) were established by adding 750 μl of a 1% (wt/vol) high-melt agarose containing a plug (height approx. 5 mm) of FeS, $FeCO_3$, $FeCl_2$ or by spreading ZVI (200 mesh; metal basis; Alfa Aesar, Ward Hill, MA) at the bottom of the glass vial, in this latter case, no high melt agarose was used. FeS was synthesized in a modified way as described by Kucera and Wolfe (1957) by reacting equimolar amounts of sulfide with Fe(II) using $Na_2S \times 9H_2O$ and $FeSO_4 \times 7\ H_2O$. After being separately dissolved in 80°C anoxic deionized water (Milli-Q Integral System, Merck Millipore), the $FeSO_4$ solution was quickly added to the Na_2S solution resulting in instantaneous precipitation of FeS. This precipitate was allowed to settle overnight. The supernatant of the settled FeS was washed two to three times with each time 2 L warm anoxic distilled water (~80–90°C) until the water above the FeS looked clear and had a pH around neutrality.

$FeCO_3$ was synthesized by reacting equimolar amounts of Fe(II) chloride with sodium bicarbonate. The Fe(II)-source was overlaid by 3.75 ml of a 0.15% (wt/vol) low-melt agarose containing semisolid mineral salt medium of either modified Wolfe's mineral medium (MWMM) or artificial seawater medium (ASW), including 1 ml L^{-1} of 7-vitamin- (Pfennig 1978), SL10- (Tschech and Pfennig 1984) and selenite-tungstate (Tschech and Pfennig 1984) solutions. The media were buffered with 10 mM bicarbonate and the pH was adjusted to 6.5 by stepwise addition of 1 M HCl and constantly checking the pH with a pH electrode. MWMM contained of the following salts per liter: 0.1 g NH_4Cl, 0.2 g $MgSO_4 \times 7\ H_2O$, 0.1 g $CaCl_2 \times 2\ H_2O$ and 0.05 g K_2HPO_4. Per liter, ASW was composed of 17.3 g NaCl, 8.6 g $MgCl_2 \times 6\ H_2O$, 0.025 g $MgO_4 \times 7\ H_2O$, 0.996 g $CaCl_2 \times 2\ H_2O$, 0394 g KCl, 0.059 g KBr, 0.25 g NH_4Cl and 0.05 g K_2HPO_4. For comparison, a batch of $FeCO_3$ was prepared following the protocol of Hallbeck, Ståhl and Pedersen (1993) using $Fe(NH_4)SO_4$ and Na_2CO_3 instead of $FeCl_2$ and $NaHCO_3$ for synthesis. The tubes were prepared anoxically and opened the first time during inoculation with bacteria one day after preparation, leading to an air-filled headspace.

The tubes were inoculated under sterile conditions with 50 μl, which was a tenfold diluted sample from another gradient tube and incubated at 20°C in the dark. An Fe(II)-oxidizing culture dominated by *Betaproteobacteria* (belonging to *Gallionella* sp.) and with minor traces of *Alphaproteobacteria* (belonging to *Azorhizobium* sp.) enriched from a freshwater sediment (Lake Constance, N 47° 41′42.63″; E 9° 11′ 40.29″, Germany) was selected and a culture of a marine Fe(II)-oxidizer, belonging to the *Zetaproteobacteria* (98% homolog to *Mariprofundus* sp. M34), isolated from sediment from Aarhus Bay (N 56° 16.811′; E 010° 28.056′; Baltic Sea, Denmark) was used as marine Fe(II)-oxidizer representative (Laufer *et al.* 2016). The negative control was treated in a similar way without inoculation. Growth of bacteria was defined as positive if brownish accumulations that spread out from the inoculum could visually be observed and clear differentiation from the negative control could be done (Emerson and Floyd 2005). This will henceforth be called Fe(III) mineral accumulations.

Cell counts

Bacterial cells in the top layers of freshly prepared MWMM with FeS gradient tubes were counted by fluorescent microscopy in triplicates at each time point to demonstrate bacterial growth. For cell counts, the top layer of the gradient tubes was centrifuged and the cell-mineral pellet was resuspended in 1.5 ml of 10 mM bicarbonate buffer. Paraformaldehyde at a final concentration of 2% was added and the samples were stored at 4°C until analysis. One ml of this suspension was added to 9 ml of oxalate solution (28 g L^{-1} ammonium oxalate and 15 g L^{-1} oxalic acid) to dissolve the Fe(III) minerals and further tenfold diluted in oxalate solution. Ten ml were then filtered onto a white GVWP filter (Millipore, 0.22 μm) and 1 μg ml^{-1} DAPI stain was used to stain the cells. Cells were counted using a Leica DM5500B fluorescent microscope using the A4 filter.

Geochemical measurements

Geochemical measurements were always performed in the same gradient tubes using microsensors at 20°C. For each setup, two gradient tubes were inoculated and two additional gradient tubes were prepared as negative control. Concentration profiles were performed only once in every gradient tube at each time point to disturb the system as little as possible. O_2 concentration depth profiles were measured with a 100 μm tip diameter amperometric Clark-type O_2 microelectrode (Unisense, Aarhus, Denmark) as described by Revsbech (1989). A two-point calibration was done in air-saturated and in anoxic water. Vertical O_2 profiles in gradient tubes were recorded in triplicates in depth intervals of 0.5 mm using a motorized micromanipulator (Unisense) and used for the calculation of O_2 consumption rates using the program PROFILE 1.0 (Berg Risgaard-Petersen and Rysgaard 1998). The O_2 concentration measured at the top of the top layer (depth 0 mm) was chosen as first boundary condition, an O_2 flux at the bottom of the tube (21 mm) of 0 μmol dm^{-2} s^{-1} was set as second boundary condition and an O_2 diffusion coefficient of $2.4 \cdot 10^{-9}$ m^2 s^{-1} (McMillan and Wang 1990) was used.

All microsensor data for measurements in gradient tubes were plotted as follows: depth 0 mm refers to the atmosphere/top layer (agar) interface, and the surface of the Fe(II)-source is located at approx. 21 mm. The time between the single measurement time points are 1 (t_0 – t_3) and 3 days (t_3 – t_6).

Fe^{2+} concentration depth profiles were determined by voltammetry using a DLK-100A potentiostat (Analytical Instrument Systems, Flemington, NJ) with a standard three-electrode system. The working electrode, a glass-encased 100 μm gold amalgam (Au/Hg) electrode, was constructed as described by Brendel and Luther (1995). The reference electrode was a solid-state Ag wire coated in Ag/AgCl; a Pt wire was used as counter electrode. Working and reference electrode were re-plated before every daily measurement. Fe^{2+} calibrations were done using Mn^{2+} standards with subsequent conversions to Fe^{2+} concentrations using the pilot ion method (Brendel and Luther 1995; Slowey and Marvin-DiPasquale 2012). A conversion factor from Mn^{2+} to Fe^{2+}, called pilot ion factor was determined to be 1.3. For this, a proper calibration for Fe^{2+} and Mn^{2+} was performed in an anoxic glovebag to prevent any Fe^{2+} oxidation. The slopes of the calibrations were then divided by each other (Mn^{2+}/Fe^{2+}). The determined conversion factor was later used for any calibrations that have been performed with Mn^{2+} prior to measurements. Cyclic voltammetry was performed for the detection of Mn^{2+} and Fe^{2+} at 1000 mV s^{-1} between −0.1 and −2.0 V (freshwater) or −1.8 V (seawater) vs Ag/AgCl. An initial conditioning step of applying −0.05 V for 5 s followed by holding −0.9 V for 10 s were set to remove previously deposited species (Brendel and Luther 1995). After the conditioning steps, the electrode equilibrated for 5 s before scan potentials were applied. 10 scans were run at each measurement point, the final 3 voltammograms were integrated using VOLTINT program for Matlab® (Bristow and Taillefert 2008). Data were recorded in 4 mm depth intervals using a manual micromanipulator (Unisense, Aarhus, Denmark). Fe^{2+} consumption rates were not calculated because the low amount of data points led to statistically invalid results.

Energetic and kinetic calculations

The overall reaction of homogeneous oxidation of Fe^{2+} by dissolved O_2 to Fe^{3+} and further precipitation as Fe(III) hydroxide can be summarized as (Roden *et al.* 2004)

$$Fe^{2+} + 0.25\ O_2 + 2.5\ H_2O \rightarrow Fe(OH)_3 + 2\ H^+ \quad (1)$$

Values of Gibbs free energy ΔG of this reaction in different depths and time points were calculated according to

$$\Delta G = \Delta G_0 + R \cdot T \cdot InQ \quad (2)$$

with ΔG_0 as the standard Gibbs free energy of the reaction (−109 kJ mol^{-1} (Roden *et al.* 2004)), R as the ideal gas constant, T as the temperature in Kelvin and Q as the activity product of the reaction.

Considering homogeneous Fe^{2+} oxidation only, the kinetic rate law for neutral solutions then is

$$-\frac{d[Fe^{2+}]_{hom}}{dt} = k \cdot [Fe^{2+}] \quad (3)$$

with $k = k_0 \cdot [O_2] \cdot [OH^-]^2$ and the universal rate constant for homogeneous Fe^{2+} oxidation by O_2 k_0 being $2.3 \cdot 10^{-14}$ mol^3 L^{-3} s^{-1} at 25°C (Tamura Goto and Nagayama 1976). The total general rate equation of Fe^{2+} oxidation considering both, homogenous and heterogeneous oxidation, was found to be (Tamura Goto and Nagayama 1976)

$$-\frac{d[Fe^{2+}]}{dt} = (k + k' \cdot [Fe(III)]) \cdot [Fe^{2+}] \quad (4)$$

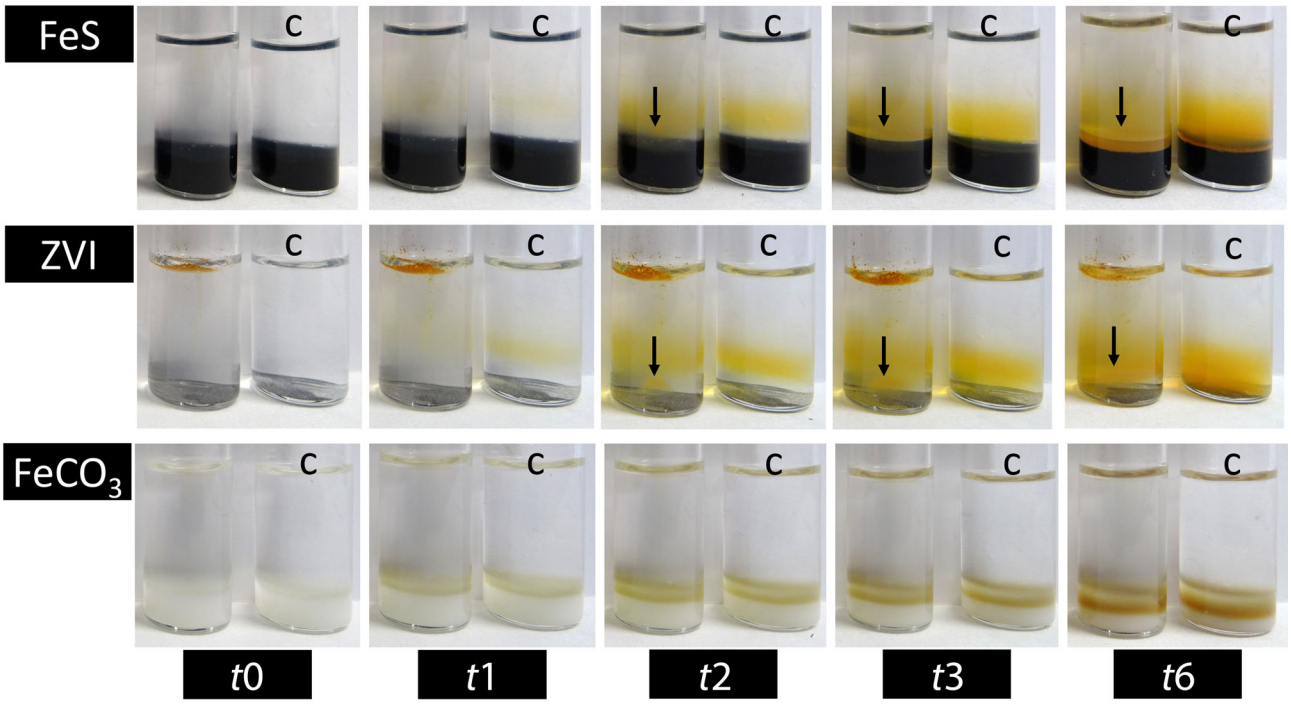

Figure 1. Images of the temporal development of negative control (c) and inoculated MWMM gradient tubes with an enrichment of freshwater microaerophilic Fe(II)-oxidizers from Lake Constance, Germany, with the Fe(II)-sources FeS, ZVI and $FeCO_3$ starting at the day of inoculation (t_0). Growth in FeS and ZVI gradient tubes is indicated by formation of sharp orange Fe(III) mineral accumulations within or below the orange colored top layer of the gradient tubes highlighted in the image with an arrow. Neither growth nor abiotic Fe(II) oxidation could be observed in $FeCO_3$ tubes within the top layer, only directly on the $FeCO_3$ plug at the bottom, indicated by a color change to brown. (t_1 = day 1, t_2 = day 2, t_3 = day 3 and t_6 = day 6 after inoculation)

Heterogeneous Fe^{2+} oxidation is accelerated by Fe(III) minerals (Tamura Kawamura and Hagayama 1980). The amount of Fe(III) hydroxide precipitated is equal to the amount of oxidized Fe^{2+} (Tamura Goto and Nagayama 1976); therefore, [Fe(III)] in the gradient tube top layer at any time can be calculated by

$$[\mathrm{Fe\,(III)}] = [\mathrm{Fe^{2+}}]_{t0} - [\mathrm{Fe^{2+}}] \quad (5)$$

The rate law of heterogeneous Fe^{2+} oxidation can be described as

$$-\frac{d[\mathrm{Fe^{2+}}]_{het}}{dt} = k' \cdot [\mathrm{Fe\,(III)}] \cdot [\mathrm{Fe^{2+}}] \quad (6)$$

with $k' = \frac{k_{s,0} \cdot [O_2] \cdot K}{[H^+]}$ and the specific rate constant for the heterogeneous reaction $k_{s,0}$ being 73 mol L^{-1} s^{-1} (Tamura Goto and Nagayama 1976) and the dimensionless adsorption constant of ferrous iron on ferric hydroxide K being $10^{-4.85}$ (Sung and Morgan 1980). Additionally, half-life for Fe^{2+} oxidation in the gradient tubes was calculated by equations (7) and (8) for homogenous or heterogeneous Fe^{2+} oxidation, respectively

$$t_{\frac{1}{2},hom} = \frac{\ln(2)}{k} \quad (7)$$

$$t_{\frac{1}{2},het} = \frac{\ln(2)}{k' \cdot [\mathrm{Fe\,(III)}]} \quad (8)$$

The energetic and kinetic calculations were exemplarily done for gradient tubes containing MWMM and FeS as Fe(II)-source.

RESULTS

Comparison of different Fe(II)-sources for suitability of growth of microaerophilic Fe(II)-oxidizers

We found that both FeS and ZVI are suitable Fe(II)-sources for the cultivation of freshwater and marine microaerophilic Fe(II)-oxidizers in opposed Fe^{2+}-O_2 gradient tubes using agar as a stabilizing agent. In these gradient tubes, a diffuse orange-brownish smear was observed 1 day after inoculation in the center of the top layer in inoculated as well as in negative control tubes (for both MWMM and ASW medium) (Fig. 1). First distinct Fe(III) mineral accumulations appeared 2–3 days (freshwater Fe(II)-oxidizers) and 5–6 days after inoculation (marine Fe(II)-oxidizers), respectively. Cell counts in freshly prepared gradient tubes containing MWMM and FeS clearly demonstrated an increasing cell number and thus microbial growth in the area of the distinct Fe(III) mineral accumulations (Fig. 2). Depending on the identity of Fe(II)-source and the identity of the inoculated bacteria, the shape and the height of the formed distinct Fe(III) mineral accumulation (often described in the literature as band formations) can be different (Fig. 3), including flat plane (Fig. 3A and D), funnel-like (Fig. 3C and E), curved plane (Fig. 3B) and cloud structures (Fig. 3F).

In addition to these setups, ZVI was stabilized in a 1% high melt agarose bottom layer so the ZVI was not in direct contact with the low melt agarose where the bacteria grew. In this case, accumulations of Fe(III) minerals were observed only in minor amounts at the surface of the bottom layer (image not shown). Similar to the gradient tubes that contained $FeCO_3$ (mineral prepared following two different protocols) and $FeCl_2$ as Fe(II)-source, this setup did not reveal significant growth of Fe(II)-oxidizing bacteria (data not shown). The Fe(II)-sources in

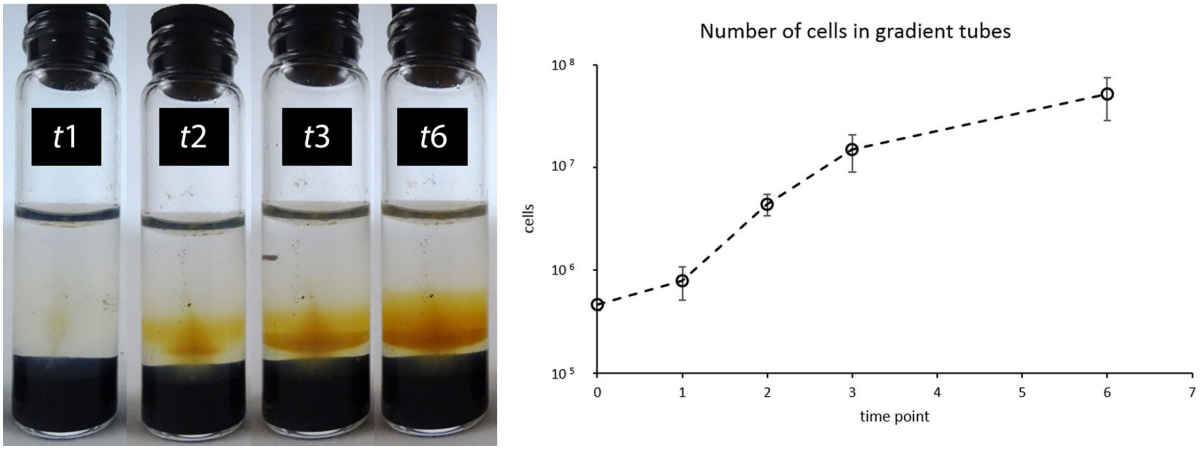

Figure 2. Cell numbers in gradient tubes containing MWMM and a FeS bottom layer at different time points ((t_1 = day 1, t_2 = day 2, t_3 = day 3 and t_6 = day 6 after inoculation). An image showing the development of the Fe(III) mineral accumulations in the top layer is shown on the left side. The gradient tubes for cell counts were freshly prepared and are comparable to the tubes, in which the geochemical O_2 and Fe^{2+} measurements were performed in. Error bars show the standard deviation of the counted triplicates.

gradient tubes that contained $FeCO_3$ as bottom layer got oxidized within a day after inoculation (Fig. 1) and therefore did not show any Fe^{2+} gradients across the top layer. A similar absence of Fe^{2+} gradients was obtained for tubes that had been kept anoxically for 2 days in order to provide optimal conditions for the establishment of a pronounced Fe^{2+} gradient across the top layer. Spectrophotometric quantification of dissolved Fe(II) (ferrozine assay) revealed only low concentrations of Fe^{2+} compared to water saturation (approximately 50 μM, data not shown). The mineralogical identity of $FeCO_3$ was verified by Mössbauer spectroscopy analysis (data not shown). $FeCl_2$ gradient tubes were set up with different concentrations in the bottom layer (1 mM, 500 μM, 200 μM). In none of these tubes were Fe(III) mineral accumulations observed. A summary of the observations is listed in Table 1.

Geochemical depth profiles

Exemplary O_2 concentration depth profiles from gradient tubes inoculated with an enrichment of freshwater Fe(II)-oxidizers from Lake Constance (Fig. 3A and B) or with a marine isolate from Aarhus Bay (Fig. 3C) are shown in Fig. 4. The O_2 concentration decreased in all tubes towards the bottom of the tube. No O_2 reached the bottom of tubes during the day of inoculation (t_0) (Fig. 4). O_2 concentrations increased over time over the whole depth until stabilization beginning at t_2 (day 2; ZVI tubes) or t_3 (day 3; FeS tubes). At t_2, the first distinct Fe(III) mineral accumulations were formed in the inoculated FeS freshwater tubes at a depth of around 16 mm, corresponding to an O_2 concentration of approx. 20 μM. No O_2 was detected at t_2 below these accumulations, which were close to the Fe(II)-source at the bottom of the tube (Fig. 4A). In the ZVI freshwater tubes, Fe(III) minerals also accumulated at t_2 at a depth of approximately 18 mm. The temporal shifts of the O_2 distribution throughout the tubes containing ASW (Fig. 4C and D) mirror the trend that was observed in tubes containing MWMM (Fig. 4A and B). In all tubes the spatial O_2 distribution profiles shift from a concave to a linear shape over time, which reflects the shift of dominant O_2 consumption zones from top to bottom of the tubes (Fig. 5). O_2 concentrations were slightly lower in ASW setups. During the entire experiment, significant differences in O_2 concentrations between negative control tubes and inoculated tubes were observed only during short time frames, e.g. at t_2 in freshwater FeS tubes (Fig. 4A).

Emerson and Moyer (1997) noted a depletion of O_2 in the headspace of inoculated gradient tubes. Renewing the headspace by opening the tube again led to the formation of a second growth band consisting of Fe(III) mineral accumulations below the already grown first band. In the present study, the tubes were opened daily to measure the O_2 concentrations, which led to a frequent regeneration of the headspace in the tubes. To ensure that the renewed headspace had no influence on the O_2 concentrations in the top layer, additional tubes were prepared that were all inoculated at the same time and just opened once again when they were measured. They did not have significantly lower O_2 concentrations than the tubes that were opened daily for measurements (data not shown). This also shows that no significant additional O_2 entered the top layer by the microelectrode insertion or removal.

O_2 consumption rates for gradient tubes containing MWMM and FeS are shown in Fig. 5. Consumption rates in the other gradient tubes that have been used for measurements were in a similar order of magnitude (0–12 nmol L^{-1} s^{-1}). Over time, the O_2 consumption shifted in all gradient tubes down towards the bottom of the tube. After 3–4 days, O_2 was only consumed below 15 mm in the top layer with O_2 consumption rates of below 10 nmol L^{-1} s^{-1}. No significant differences in O_2 consumption were observed between negative control tubes and inoculated tubes.

Exemplary Fe^{2+} concentration depth profiles are shown in Fig. 6. The highest Fe^{2+} concentrations were measured at the bottom of all tubes with decreasing concentrations upwards. At t_0, Fe^{2+} concentrations of about 2.5 μM were measured directly above the bottom layer in freshwater FeS tubes (Fig. 6A). Fe(III) mineral accumulations were visually observed starting at t_2. First mineral accumulation appeared in the center of the tube (right at the inoculation funnel) and spread in all directions with Fe^{2+} concentrations of approximately 300–400 μM. From t_0 to t_2, an additional peak in the voltammograms at $E_{1/2}$ = −1.1 V vs. Ag/AgCl in depths below 12 mm depth was detected in the cathodic wave that was identified as $FeS_{(aq)}$ signal. These data could not be quantified due to a lack of standards for $FeS_{(aq)}$ (Davison Buffle and DeVitre 1998; Luther *et al.* 2003; Ciglenecki

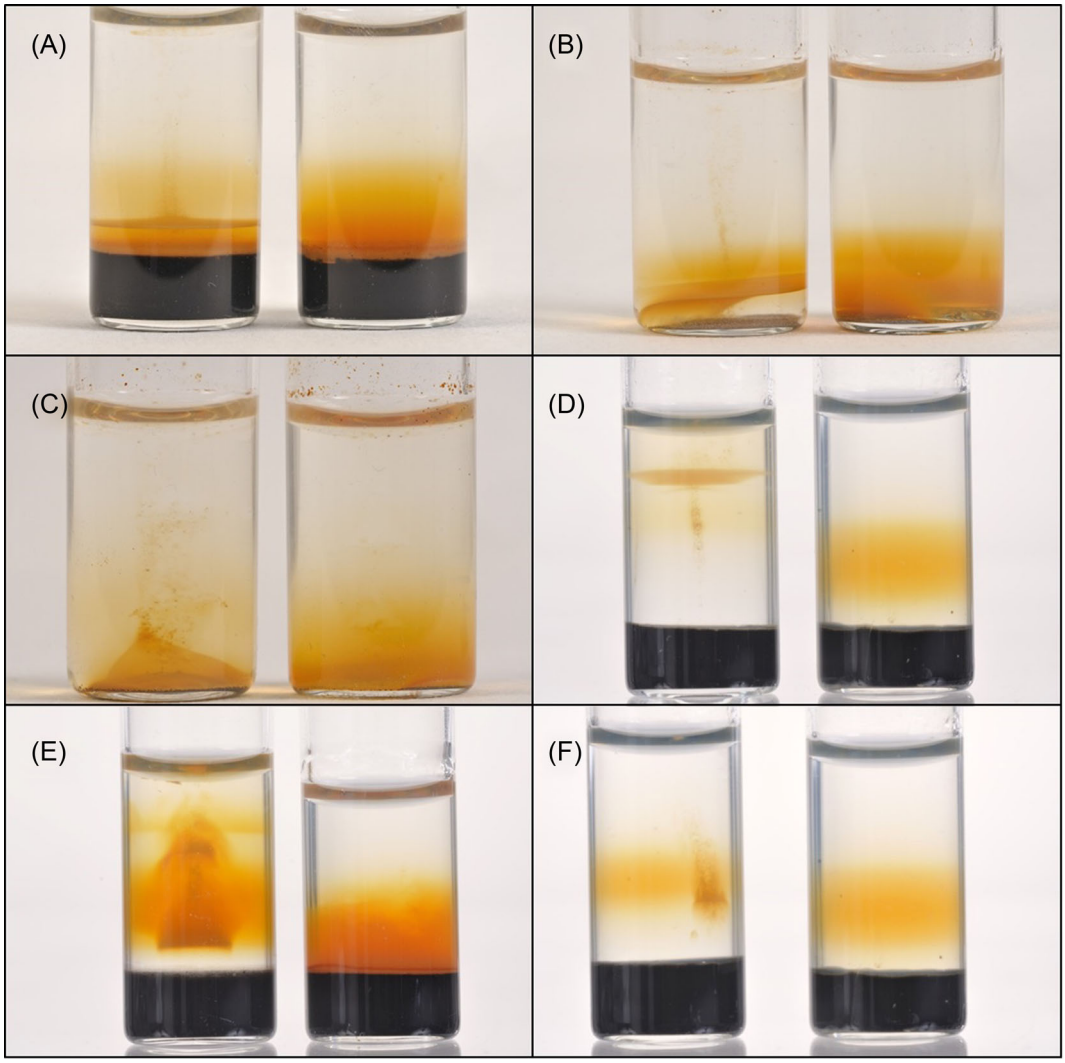

Figure 3. Images of inoculated (left tube) and negative control gradient tubes (right tube) with microaerophilic Fe(II)-oxidizers from different field sites, media and Fe(II)-sources at different time points. (**A**) freshwater lake sediment enrichment (Lake Constance), MWMM, FeS, 8 days after inoculation; (**B**) freshwater lake sediment enrichment (Lake Constance), MWMM, ZVI, 8 days after inoculation; (**C**) marine sediment isolate (Aarhus Bay, Denmark), ASW, ZVI, 31 days after inoculation; (**D**) freshwater ditch, MWMM, FeS, 3 days after inoculation; (**E**) sample from peat canal, MWMM, FeS, 17 days after inoculation; (**F**) isolate from microbial mat in a mine (Black Forest, Germany), MWMM, FeS, 3 days after inoculation. The dimensions of the tube are: height 6.1 cm, diameter 1.7 cm.

et al. 2014). This leads to some underestimation of total dissolved Fe^{2+} concentrations in these tubes. Similar to the FeS tubes, Fe(III) mineral accumulations in freshwater ZVI tubes were observed from t_2 in regions with about 300–400 μM Fe^{2+}. In gradient tubes containing ASW and a FeS bottom layer, a small extent of Fe(III) mineral accumulations was observed at t_6 directly at the bottom of the tubes, where Fe^{2+} concentrations of approximately 100–200 μM were measured. No significant differences in measured Fe^{2+} concentrations between negative control tubes and inoculated tubes were measured. In gradient tubes with ASW and ZVI as Fe(II)-source, first Fe(III) mineral accumulations appeared at t_1 in regions with about 500–700 μM Fe^{2+}. In general, Fe^{2+} concentrations decreased over the time of the experiment. Higher Fe^{2+} concentrations were generally measured in gradient tubes using FeS as Fe(II)-source. The gradients in negative control tubes and inoculated tubes were with some exceptions very similar (Fig. 6).

Calculations using Gibbs free energy show potentially higher energy for the metabolism of Fe(II)-oxidizing bacteria during Fe(II) oxidation at greater depths within the top layers of the gradient tubes (Fig. 7A). However, the amount of energy that can be obtained decreases with time. Kinetic calculations reveal higher rates of homogeneous Fe(II) oxidation near the top layer headspace interface (depth 0 mm) due to higher O_2 concentrations and consequently a shorter half-life of Fe^{2+} in solution (Fig. 7B and C). A comparison between homogeneous and heterogeneous Fe(II) oxidation rates in 16 mm depth of the top layer exhibit a rapid overtaking of the heterogeneous oxidation leading to a dramatic decrease of Fe^{2+} half-life times from t_1 in this depth (Fig. 7D).

DISCUSSION

Suitability of different Fe(II)-sources for cultivation in gradient tubes

In this study, we have compared the suitability of the different Fe(II)-sources FeS, $FeCO_3$, ZVI and $FeCl_2$ for the cultivation of freshwater and marine microaerophilic Fe(II)-oxidizers in agar-stabilized gradient tubes. Although successful growth has been

Table 1. Summary of observations in opposed gradient tubes with different Fe(II)-sources.

Fe(II)-source	Diffuse orange smear in the top layer	Characteristic appearance of the Fe(III) mineral accumulations
FeS	- Started 1 day after inoculation in all tubes - Started in the center of the top layer - Extent increased towards top and bottom	MWMM: observed 2 days after inoculation as sharp flat band a few mm above the bottom layer ASW: observed 5 days after inoculation as cloudy, colony-like accumulations close to or directly on the bottom layer
ZVI without additional agarose plug	- Started 1 day after inoculation in all tubes - Started in the center of the top layer - Extend increased to top and bottom	MWMM: observed 2 days after inoculation as sloping bands a few mm above the ZVI powder ASW: observed 5–6 days after inoculation as sloping bands almost directly on ZVI powder
ZVI inserted in bottom layer	- Started 3 days after inoculation in all tubes - Only in regions close to the bottom layer	MWMM: observed 3 days after inoculation as darker orange color compared to the negative control directly on the surface of the bottom layer ASW: observed 5 days after inoculation starting as small colonies directly on the surface of the bottom layer
$FeCO_3$	Not observed	No mineral accumulations were formed
$FeCl_2$	Not observed	No mineral accumulations were formed

reported in the literature for all Fe(II)-sources (Emerson and Moyer 1997; Sobolev and Roden 2001; Neubauer Emerson and Megonigal 2002; Edwards *et al.* 2003; Weiss *et al.* 2007; Druschel *et al.* 2008; McBeth *et al.* 2011; Swanner Nell and Templeton 2011; Kato *et al.* 2012; Kato *et al.* 2013; MacDonald *et al.* 2014; Laufer *et al.* 2016), in the present study we have only observed the formation of orange Fe(III) (oxyhydr)oxide minerals using FeS and ZVI. In $FeCl_2$ and $FeCO_3$ tubes, no diffusion of Fe^{2+} was observed into the top layer, leading to the lack of the orange band and no growth of microaerophilic Fe(II)-oxidizers. We could show that $FeCO_3$ and $FeCl_2$ are highly sensitive in handling with respect to stability and oxygen sensitivity. Minor variations in handling and preparation cause failure of the method. Rapid oxidation directly at the Fe(II) plug confirmed that chemical oxidation by O_2 prevents the establishment of an Fe^{2+} gradient throughout these $FeCl_2$ and $FeCO_3$ tubes. These observations are in agreement with geochemical properties of these Fe(II) phases. The $FeCO_3$ solubility at room temperature and low ionic strength has been shown to be in the range of 3.72×10^{-11} to 9.33×10^{-12} $mol^2\ L^{-2}$ (Sun Nešić and Woollam 2009). The fast rate of chemical Fe^{2+} oxidation, combined with the low solubility of $FeCO_3$ and low diffusion of Fe^{2+} (0.719×10^{-9} $m^2\ s^{-1}$ (Lide 2008)) leads to rapid depletion of Fe^{2+} in the top layer of gradient tubes. The solubility product of FeS has been determined to be significantly higher, in the range of $10^{-2.95}$ (amorphous FeS) (Davison 1991) to $10^{-3.5}$ (Rickard and Luther 2007). Increasing solubility of the Fe(II) minerals enhances the diffusion of Fe^{2+} into the top layer. However, an accurate estimation of released Fe^{2+} to the top layer from the FeS bottom plug is impossible, as the mineral ageing of FeS (including Ostwald ripening and mineral transformation) significantly affects FeS solubility.

Few studies reported on the successful growth of microaerophilic Fe(II)-oxidizers in gradient tubes using $FeCO_3$ as Fe(II)-source (Emerson and Moyer 1997; Swanner Nell and Templeton 2011; Emerson *et al.* 2013; MacDonald *et al.* 2014; Field *et al.* 2016; Chiu *et al.* 2017). In these studies, $FeCO_3$ was synthesized following the protocol of Hallbeck, Ståhl and Pederse (1993). Following this procedure, we revealed similar results compared to the use of $FeCO_3$ that was prepared after our lab protocol. This confirms the high sensitivity of this mineral for the application as Fe(II)-source for gradient tubes, using $Fe(NH_4)SO_4$ and Na_2CO_3 instead of $FeCl_2$ and $NaHCO_3$ for synthesis. In these studies, it was also noted that only fresh $FeCO_3$ could be used, since the $FeCO_3$ lost potency to release Fe^{2+} within one week.

$FeCl_2$ concentrations used in this study (1 mM, 500 μM and 200 μM) were low compared to those used by Sobolev and Roden (50 mM) (2001). They used concentrations that were much too high (50 mM) compared to concentrations observed in natural systems in a 250 ml beaker overlaid by a 125 ml top layer to sustain an environmentally relevant Fe^{2+} flux over the course of the experiment. As the glass vials used in this study only have a small volume of 8 ml, lower Fe(II) concentrations were chosen. Higher $FeCl_2$ concentrations (up to 10 mM) as iron source in the bottom layer were tested for the growth of microaerophilic Fe(II)-oxidizers (data not shown); however, no distinct Fe(III) mineral accumulations (that are linked to biotic Fe(II) oxidation) were observed in any of them. Only a fast color change to orange could be seen in the top layer, which is related to fast chemical oxidation.

A comparison between FeS and ZVI tubes showed that both Fe(II)-sources worked equally well for cultivation of both freshwater and marine microaerophilic Fe(II)-oxidizers. The method to use ZVI as Fe(II)-source in gradient tubes was used for marine strains as the corrosion rates are expected to be higher due to higher ionic strength. However, few studies using ZVI had success with freshwater strains ((Kato *et al.* 2012), this study). In ZVI gradient tubes, distinct Fe(III) mineral accumulations indicating growth of Fe(II)-oxidizers occurred sometimes slightly earlier than in FeS tubes. Finally, the differences in the gradient tubes are dependent on the physico-chemical parameters of the Fe(II)-source and the gradient tube medium. A higher solubility of the Fe(II)-source generally leads to steeper diffusion gradients and consequently to faster diffusion of Fe^{2+} into the top layer.

The position and the shape of the Fe(III) mineral accumulations in FeS tubes inoculated with different bacterial strains varied. Emerson and Floyd (2005) pointed out that every batch of

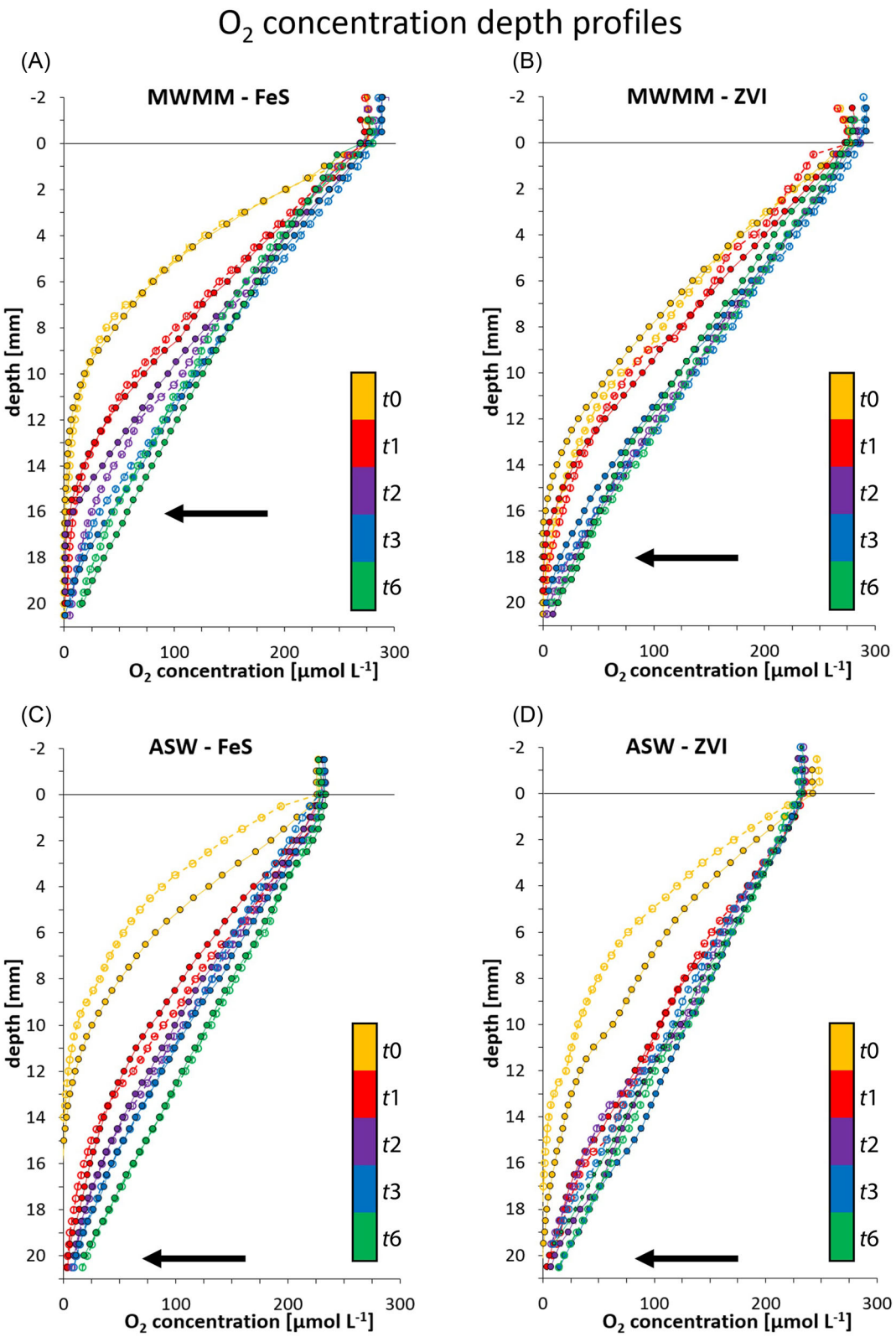

Figure 4. Selected O_2 concentration depth profiles in gradient tubes inoculated with an enrichment of freshwater microaerophilic Fe(II)-oxidizers from Lake Constance, Germany (A,B) or with an isolate of a marine Fe(II)-oxidizer from Aarhus Bay, Denmark (C,D). Open symbols and dashed lines represent negative control tubes, closed symbols and solid lines inoculated tubes. Error bars are not shown as the mean coefficient of variation of all profiles is below 3%. The colors display the different times of measurements starting the day of inoculation (t_0). Depth 0 mm shows the headspace-top layer interface; the Fe(II)-source starts in a depth of about 21 mm. The arrow indicates the approximate level where the growth band formed in inoculated tubes. (**A**) Gradient tubes with MWMM and FeS bottom layer; (**B**) Gradient tubes with MWMM and ZVI powder at the bottom; (**C**) Gradient tubes with ASW and FeS bottom layer; (**D**) Gradient tubes with ASW and ZVI powder at the bottom. (t_1 = day 1, t_2 = day 2, t_3 = day 3 and t_6 = day 6 after inoculation)

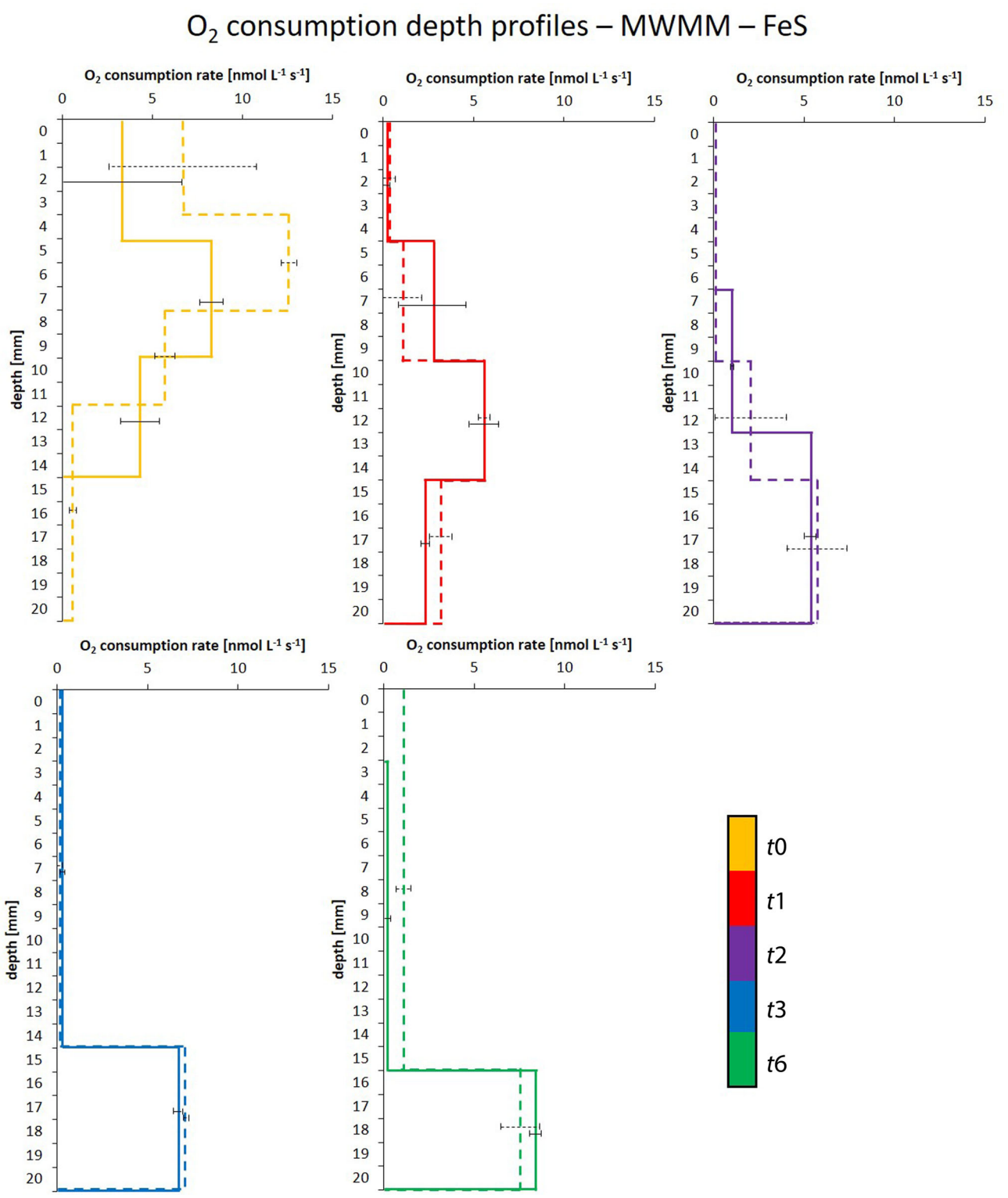

Figure 5. O_2 consumption profiles for gradient tubes for negative control tubes (dashed lines) and inoculated tubes (solid lines) for different measurement time points (t_0 = day of inoculation, t_1 = day 1, t_2 = day 2, t_3 = day 3 and t_6 = day 6 after inoculation) in gradient tubes containing MWMM and a FeS bottom layer that starts at a depth of approx. 21 mm. Error bars show the minimum and maximum of the duplicate O_2 concentration measurements. Data were obtained using PROFILE 1.0. Oxygen consumption rates in inoculated tubes in the first 3 mm at t_6 are not shown due to falsified data resulting from irregularly measured O_2 concentrations at this depth. The differences in O_2 consumption between negative control and inoculated tubes at t_0 occurred through the temporal distance and between the measurements and the influence of the fast diffusion.

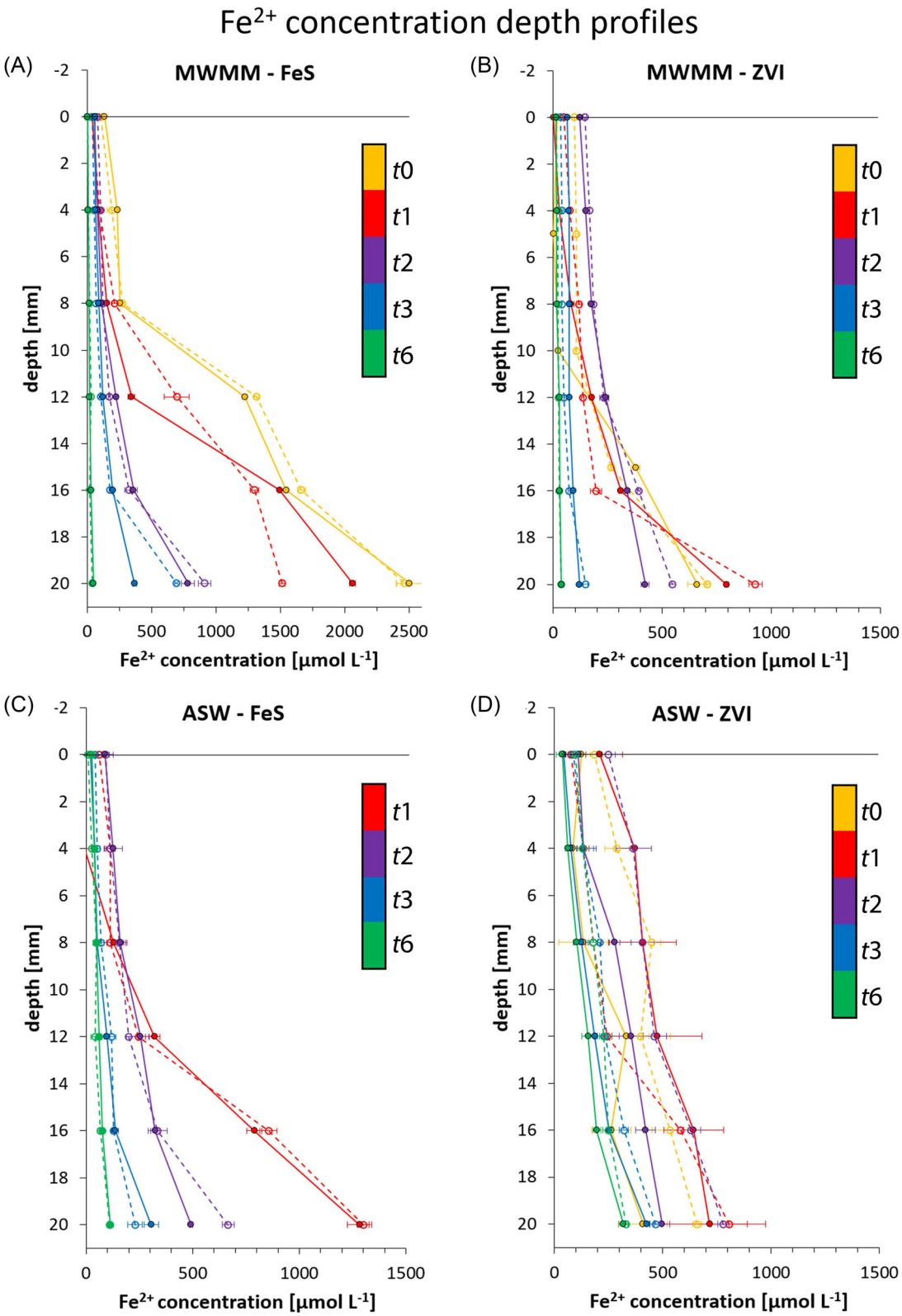

Figure 6. Selected Fe^{2+} concentration depth profiles for gradient tubes inoculated with an enrichment of freshwater microaerophilic Fe(II)-oxidizers from Lake Constance, Germany (**A**) and (**B**) or with an isolate of a marine Fe(II)-oxidizer from Aarhus Bay, Denmark (**C**) and (**D**). Open symbols and dashed lines represent negative control tubes, closed symbols and solid lines inoculated tubes. Error bars show the standard deviation of the triplicate measurements. The colors display the different times of measurements starting at the day of inoculation (t_0). (**A**) Gradient tubes with MWMM and FeS bottom layer; (**B**) Gradient tubes with MWMM and ZVI powder at the bottom; (**C**) Gradient tubes with ASW and FeS bottom layer; (**D**) Gradient tubes with ASW and ZVI powder at the bottom. (t_1 = day 1, t_2 = day 2, t_3 = day 3 and t_6 = day 6 after inoculation)

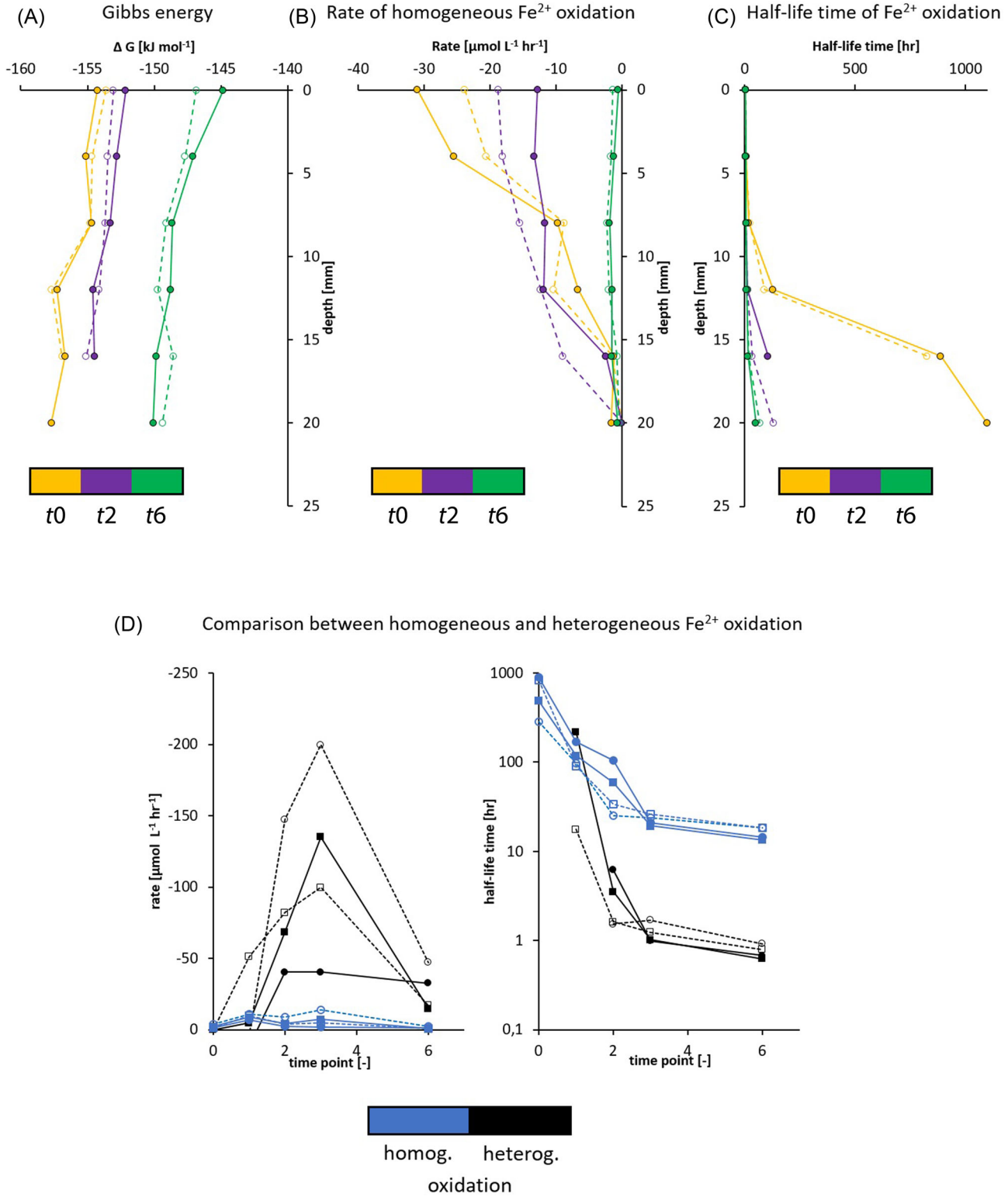

Figure 7. Representative energy, rate and half-life time profiles for gradient tubes containing MWMM and an FeS bottom layer at different time points. Open symbols and dashed lines represent negative control tubes, closed symbols and solid lines inoculated tubes. (**A**) Profiles of Gibbs free energy, (**B**) rate of homogeneous Fe^{2+} oxidation, (**C**) half-life of homogeneous Fe^{2+} oxidation, (**D**) comparison between homogeneous and heterogeneous Fe^{2+} concentration in 16 mm depth over time. The depth was chosen according to the approximate level where the growth band formed in inoculated tubes. (t_0 = day of inoculation; t_2 = day 2, t_6 = day 6 after inoculation)

FeS is slightly different and FeS loses its ability to release Fe^{2+} by aging. The quality of the FeS influences the solubility and diffusion of Fe^{2+} leading to shifts of the optimum growth zone for microaerophilic Fe(II)-oxidizers. We have observed in the past that the rate of mixing Fe(II) and sulfide, the washing procedure (frequency and length of washing steps) and the storage of the FeS determines its suitability as Fe(II)-source in gradient tubes (unpublished data). Besides that, the medium composition and the cell number and activity of the inoculated strains determine the position of the Fe(III) mineral accumulations and lead to other forms of Fe(III) mineral accumulations than the shape of the classical growth bands as shown by e.g. Emerson (Emerson and Moyer 1997; Emerson and Floyd 2005) or in Fig. 3A and D. Due to these uncertainties, a quantitative visual evaluation between different Fe(II)-sources, strains or media cannot be done. However, gradient tubes are very suitable for bacterial cultivation and geochemical determination of optimum O_2 and Fe^{2+} requirements of Fe(II)-oxidizing bacteria. The Fe(II)-sources FeS and ZVI showed the best results regarding growth of freshwater and marine microaerophilic Fe(II)-oxidizing bacteria in gradient tubes and worked reliably.

Detection of optimal geochemical conditions for the growth of microaerophilic Fe(II)-oxidizers

Microaerophilic Fe(II)-oxidizing bacteria are in direct competition to chemical Fe(II) oxidation. Druschel *et al.* (2008) pointed out that chemical Fe(II) oxidation dominates at a O_2 concentrations of 275 μM and at 50 μM the biotic Fe(II) oxidation rate was faster than the abiotic rate. This fits well to our observation that Fe(III) mineral accumulations, which are produced by Fe(II)-oxidizing bacteria, occurred first in regions of O_2 concentrations of approximately 20–40 μM (Fig. 4). As most of the Fe(III) minerals accumulated very close to the Fe(II)-source at the bottom of the gradient tubes, a characteristic bend of the O_2 profiles in inoculated gradient tubes could not be observed as seen in the literature (Emerson and Moyer 1997; Edwards *et al.* 2003; Roden *et al.* 2004) where no O_2 was detected below cell growth bands. However, the tested freshwater culture was not completely pure. This might lead to slightly different conditions. The position of the Fe(III) mineral accumulations can be explained by the solubility of the Fe(II)-source, the faster O_2 diffusion (2.4×10^{-9} m^2 s^{-1} (McMillan and Wang 1990)) compared to Fe^{2+} diffusion (0.719×10^{-9} m^2 s^{-1} (Lide 2008)), but also by the specific inoculated bacteria. The bacteria might also be responsible for the varying shapes of the Fe(III) mineral accumulations that were often not occurring as typical flat band by potential formation of different geochemical niches with optimal growth conditions.

The results indicate that most Fe(II) gets oxidized chemically. Differences in the O_2 concentrations between inoculated and negative control tubes could be observed only in the beginning of the incubation and within a short timeframe when first Fe(III) mineral accumulations occurred (Fig. 8). This illustrates the competitive pressure of microaerophilic Fe(II)-oxidizers towards chemical Fe(II) oxidation. The main O_2 consumption zone in the gradient tubes shifts downwards relatively fast. Starting at t_2, O_2 solely is consumed in the lower part of the gradient tube and there are no significant differences in O_2 consumption between inoculated and negative control tubes, which reinforce the assumption that the microorganisms are most of the time in strong competition with the chemical O_2 consumption.

When Fe(III) minerals precipitated as a result of microbial or homogeneous chemical Fe(II) oxidation, they serve as a catalyst for further chemical Fe(II) oxidation (autocatalysis) and increase the rate of chemical Fe(II) oxidation (Stumm and Sulzberger 1992; Park and Dempsey 2005; Melton *et al.* 2014). This heterogeneous Fe(II) oxidation thus increases the contribution of chemical Fe(II) oxidation to the overall Fe(II) oxidation. Energetic and kinetic constraints support the hypothesis that best growth conditions for Fe(II)-oxidizing bacteria are found to be in the proximity of the Fe(II)-source in the first days after inoculation where not only the Fe^{2+} concentration still is sufficient for bacterial growth but also more energy can be obtained from the oxidation of Fe^{2+} for the bacterial metabolisms. Additionally, the bacteria at this location have the ability to compete with the half-life of the chemical Fe^{2+} oxidation that decreases dramatically over time, especially due to heterogeneous Fe^{2+} oxidation. The agreement between the Gibbs free energy and homogeneous Fe^{2+} oxidation rate profiles (Fig. 7A and B) in abiotic and inoculated gradient tubes also indicate that most Fe^{2+} in the gradient tube top layer is abiotically depleted.

Based on differences of the shape of the O_2 profiles in the inoculated tubes and the comparison of these O_2 profiles to the control tubes, it can be concluded that significant biotic Fe(II) oxidation is only dominating in the first hours to days, when distinct Fe(III) mineral accumulations occurred, which were shown to be related to bacterial growth as demonstrated by microscopic cell counts. The number of Fe(II)-oxidizing bacteria indeed increased most (Fig. 2), when spreading of the Fe(III) mineral accumulations could visually be observed. Based on these observations, bacterial cultures should therefore be transferred shortly after occurrence of distinct Fe(III) mineral accumulations to a new gradient tube before chemical Fe(II) oxidation becomes too dominant, in order to enhance the chance for isolation of microaerophilic Fe(II)-oxidizers.

Suggestions for cultivation and isolation of microaerophilic Fe(II)-oxidizing bacteria from environmental samples

In the present study, the most suitable Fe(II)-sources for cultivation of freshwater and marine microaerophilic Fe(II)-oxidizers have been FeS and ZVI. Fe(III) mineral accumulations regularly occurred in inoculated gradient tubes using these Fe(II)-sources. Visual observations also showed that FeS and ZVI were less sensitive to chemical oxidation by O_2 than $FeCO_3$ and $FeCl_2$. The Fe(II)-sources $FeCO_3$ and $FeCl_2$ immediately began to oxidize based on the appearance of rust-colored oxides upon contact with air. However, it should be noted that using FeS or ZVI as Fe(II)-sources might stimulate the growth of other abundant microorganisms. Besides being a Fe^{2+} source, FeS might also serve as sulfide source for microaerophilic sulfide-oxidizing bacteria (Nelson and Jannasch 1983; Gevertz *et al.* 2000). If sulfate gets produced biotically in these tubes, optimal conditions for heterotrophic sulfate reducers are prevalent as well if they can use carbon from organic compounds present in the agar. Due to hydrogen gas production during Fe(0) corrosion, gradient tubes using ZVI as bottom source might enrich bacteria that are capable of using hydrogen as electron donor (Jannasch and Mottl 1985; Dannenberg *et al.* 1992; Coleman *et al.* 1993). Additionally, it should be kept in mind that agar, which is used for the stabilization of the top layer of gradient tubes, is an organic substance that could be used for growth by heterotrophic bacteria. This is especially true for marine samples, as agar is prepared from algae that naturally serve as organic carbon source for marine microorganisms. Therefore, we suggest both, short-term transfers to fresh gradient tubes, and the use of different Fe(II)-sources for isolation of microaerophilic Fe(II)-oxidizing bacteria, namely

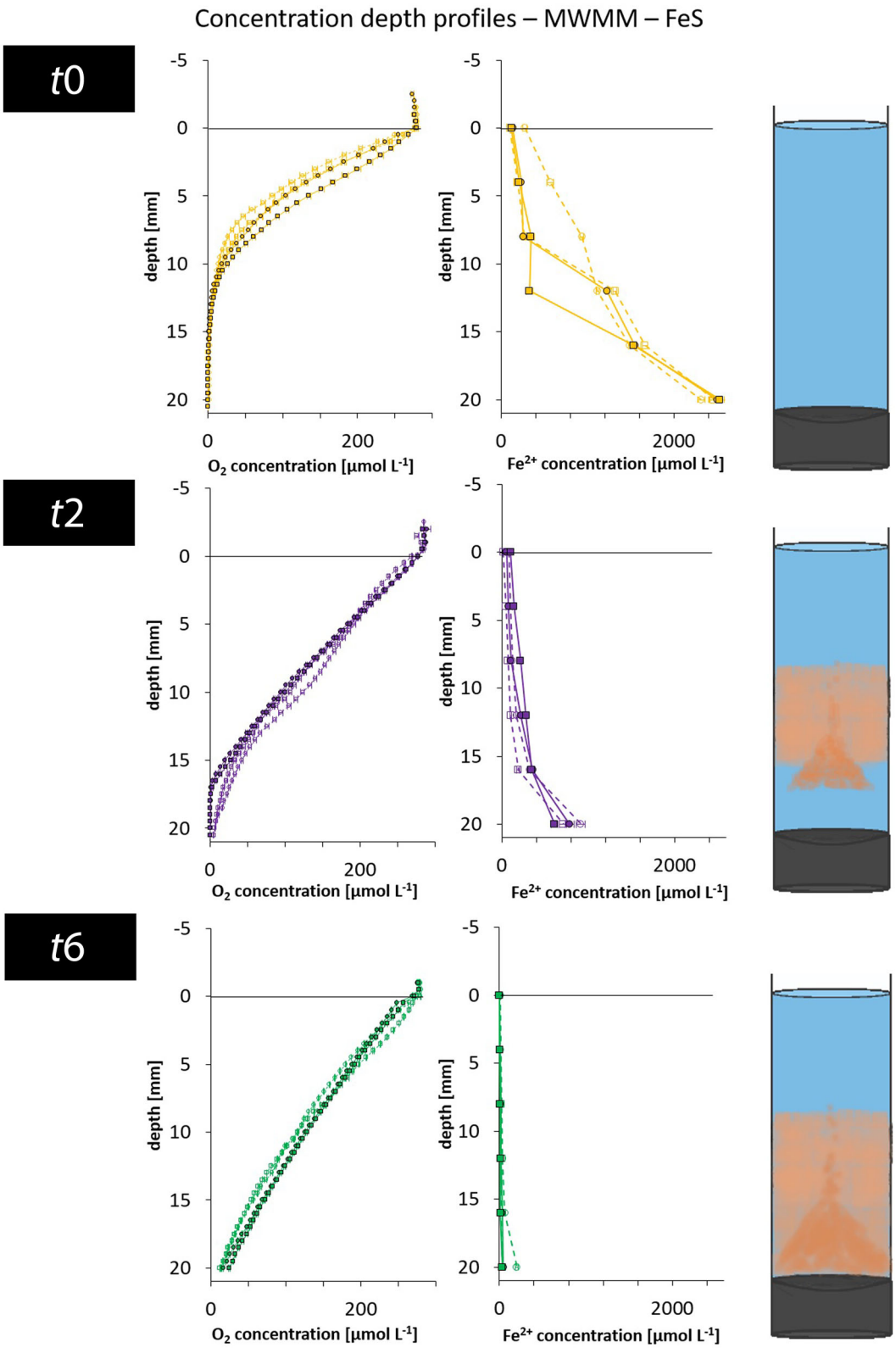

Figure 8. O_2 and Fe^{2+} concentration depth profiles for gradient tubes containing MWMM and an FeS bottom layer at t_0, t_2 and t_6 (t_0 = day of inoculation; t_2 = day 2, t_6 = day 6 after inoculation). Open symbols and dashed lines represent negative control tubes, closed symbols and solid lines inoculated tubes. Error bars show the standard deviation of the triplicate measurements. The sketches next to the profiles show the look of the gradient tubes at the respective measurement time points.

using alternating FeS and ZVI as Fe(II)-source. For enhancing the chance to remove heterotrophic bacteria from the sample, the bacterial cultures could be transferred to petri dishes containing only medium and ZVI powder (McBeth *et al.* 2011). Enrichment in the so-called gradient plates was successfully applied in the literature (Emerson and Weiss 2004; McBeth *et al.* 2011; Laufer *et al.* 2016). Freshly synthesized $FeCO_3$ according to Hallbeck, Ståhl and Pederse (1993) could also be used to suppress the growth of bacteria that are additionally feeding on substrates that are released from the Fe(II)-source, e.g. S-species. However, we recommend doing transfers between FeS and ZVI in gradient tubes and gradient plates as $FeCO_3$ is quite sensitive towards oxidation by O_2 and only poorly releases Fe^{2+}, especially if it is not freshly synthesized.

SUPPLEMENTARY DATA

Supplementary data are available at *FEMSEC* online.

ACKNOWLEDGEMENT

The authors acknowledge Katja Laufer, Elif Koeksoy, Wiebke Ruschmeier, Elizabeth Swanner and Markus Maisch for their scientific and laboratory support, as well as the donation of microaerophilic iron(II)-oxidizing strains.

FUNDING

This study was supported by a Margarete von Wrangell grant to C.S. and by the European Research Council under the European Union' s Seventh Framework Program (FP/2007– 2013)/ERC Grant, agreement number 307320 – MICROFOX to A.K.

Conflict of interest. None declared.

REFERENCES

Berg P, Risgaard-Petersen N, Rysgaard S. Interpretation of measured concentration profiles in sediment pore water. *Limnol Oceanogr* 1998;**43**:1500–10.

Brendel PJ, Luther GW. Development of a gold amalgam voltammetric microelectrode for the determination of dissolved Fe, Mn, O_2, and S(-II) in porewaters of marine and freshwater sediments. *Environ Sci Technol* 1995;**29**:751–61.

Bristow G, Taillefert M. VOLTINT: a Matlab®-based program for semi-automated processing of geochemical data acquired by voltammetry. *Comput Geosci* 2008;**34**:153–62.

Chiu BK, Kato S, McAllister SM *et al.* Novel pelagic iron-oxidizing zetaproteobacteria from the Chesapeake Bay oxic–anoxic transition zone. *Front Microbiol* 2017;**8**:1280.

Ciglenecki I, Margus M, Bura-Nakic E *et al.* Electroanalytical methods in characterization of sulfur species in aqueous environment. *J Electrochem Sci Eng* 2014;**4**:155–63.

Coleman ML, Hedrick DB, Lovley DR *et al.* Reduction of Fe(III) in sediments by sulphate-reducing bacteria. *Nature* 1993;**361**:436–8.

Cornell RM, Schwertmann U. *The Iron Oxides: Structure, Properties, Reactions, Occurrences, and Uses*. Weinheim: Wiley-VCH, 2003.

Dannenberg S, Kroder M, Dilling W *et al.* Oxidation of H_2, organic compounds and inorganic sulfur compounds coupled to reduction of O_2 or nitrate by sulfate-reducing bacteria. *Arch Microbiol* 1992;**158**:93–99.

Davison W. The solubility of iron sulphides in synthetic and natural waters at ambient temperature. *Aquat Sci* 1991;**53**:309–29.

Davison W, Seed G. The kinetics of the oxidation of ferrous iron in synthetic and natural waters. *Geochim Cosmochim Acta* 1983;**47**:67–79.

Davison W, Buffle J, DeVitre R. Voltammetric characterization of a dissolved iron sulphide species by laboratory and field studies. *Anal Chim Acta* 1998;**377**:193–203.

Druschel GK, Emerson D, Sutka R *et al.* Low-oxygen and chemical kinetic constraints on the geochemical niche of neutrophilic iron(II) oxidizing microorganisms. *Geochim Cosmochim Acta* 2008;**72**:3358–70.

Edwards KJ, Rogers DR, Wirsen CO *et al.* Isolation and characterization of novel psychrophilic, neutrophilic, Fe-oxidizing, chemolithoautotrophic α- and γ-proteobacteria from the deep sea. *Appl Environ Microbiol* 2003;**69**:2906–13.

Emerson D, Moyer C. Isolation and characterization of novel iron-oxidizing bacteria that grow at circumneutral pH. *Appl Environ Microbiol* 1997;**63**:4784–92.

Emerson D, Moyer CL. Neutrophilic Fe-oxidizing bacteria are abundant at the Loihi seamount hydrothermal vents and play a major role in Fe oxide deposition. *Appl Environ Microbiol* 2002;**68**:3085–93.

Emerson D, Weiss JV. Bacterial iron oxidation in circumneutral freshwater habitats: findings from the field and the laboratory. *Geomicrobiol J* 2004;**21**:405–14.

Emerson D, Floyd MM. Enrichment and isolation of iron-oxidizing bacteria at neutral pH. *Methods Enzymol*, 2005;**397**:112–23.

Emerson D, Field EK, Chertkov O *et al.* Comparative genomics of freshwater Fe-oxidizing bacteria: implications for physiology, ecology, and systematics. *Front Microbiol* 2013;**4**:254.

Field EK, Kato S, Findlay AJ *et al.* Planktonic marine iron oxidizers drive iron mineralization under low-oxygen conditions. *Geobiology* 2016;**14**:499–508.

Gevertz D, Telang AJ, Voordouw G *et al.* Isolation and characterization of strains CVO and FWKO B, two novel nitrate-reducing, sulfide-oxidizing bacteria isolated from oil field brine. *Appl Environ Microbiol* 2000;**66**:2491–501.

Hallbeck L, Ståhl F, Pedersen K. Phytogeny and phenotypic characterization of the stalk-forming and iron-oxidizing bacterium *Gallionella ferruginea*. *Microbiology* 1993;**139**:1531–5.

Hegler F, Posth NR, Jiang J *et al.* Physiology of phototrophic iron(II)-oxidizing bacteria: implications for modern and ancient environments. *FEMS Microbiol Ecol* 2008;**66**:250–60.

Hegler F, Lösekann-Behrens T, Hanselmann K *et al.* Influence of seasonal and geochemical changes on the geomicrobiology of an iron carbonate mineral water spring. *Appl Environ Microbiol* 2012;**78**:7185–96.

Jannasch HW, Mottl MJ. Geomicrobiology of deep-sea hydrothermal vents. *Science* 1985;**229**:717–25.

Kappler A, Straub KL. Geomicrobiological cycling of iron. *Rev Mineral Geochem* 2005;**59**:85–108.

Kashefi K, Lovley DR. Reduction of Fe(III), Mn(IV), and toxic metals at 100°C by *Pyrobaculum islandicum*. *Appl Environ Microbiol* 2000;**66**:1050–6.

Kato S, Chan C, Itoh T *et al.* Functional gene analysis of freshwater iron-rich flocs at circumneutral pH and isolation of a stalk-forming microaerophilic iron-oxidizing bacterium. *Appl Environ Microbiol* 2013;**79**:5283–90.

Kato S, Kikuchi S, Kashiwabara T *et al.* Prokaryotic abundance and community composition in a freshwater iron-rich microbial mat at circumneutral pH. *Geomicrobiol J* 2012;**29**:896–905.

Klueglein N, Zeitvogel F, Stierhof Y-D *et al.* Potential role of nitrite for abiotic Fe(II) oxidation and cell encrustation during

nitrate reduction by denitrifying bacteria. *Appl Environ Microbiol* 2014;**80**:1051–61.

Konhauser KO, Kappler A, Roden EE. Iron in microbial metabolisms. *Elements* 2011;**7**:89–93.

Kucera S, Wolfe RS. A selective enrichment method for *Gallionella ferruginea*. *J Bacteriol* 1957;**74**:344–9.

Laufer K, Nordhoff M, Røy H *et al*. Coexistence of microaerophilic, nitrate-reducing, and phototrophic Fe(II)-oxidizers and Fe(III)-reducers in coastal marine sediment. *Appl Environ Microbiol* 2016;**82**:1433–47.

Lide DR. *CRC Handbook of Chemistry and Phyics*, 88th edn. Boca Raton: CRC Press, 2008.

Lin C, Larsen EI, Nothdurft LD *et al*. Neutrophilic, microaerophilic Fe(II)-oxidizing bacteria are ubiquitous in aquatic habitats of a subtropical australian coastal catchment (ubiquitous FeOB in catchment aquatic habitats). *Geomicrobiol J* 2012;**29**:76–87.

Lovley DR, Ueki T, Zhang T *et al*. Geobacter: the microbe electric's physiology, ecology, and practical applications. *Adv Microb Physiol* 2011;**59**:1–100.

Luther GW, Glazer B, Ma S *et al*. Iron and sulfur chemistry in a stratified lake: evidence for iron-rich sulfide complexes. *Aquat Geochem* 2003;**9**:87–110.

MacDonald DJ, Findlay AJ, McAllister SM *et al*. Using in situ voltammetry as a tool to identify and characterize habitats of iron-oxidizing bacteria: from fresh water wetlands to hydrothermal vent sites. *Environ Sci Process Impacts* 2014;**16**:2117–26.

McBeth JM, Little BJ, Ray RI *et al*. Neutrophilic iron-oxidizing "zetaproteobacteria" and mild steel corrosion in nearshore marine environments. *Appl Environ Microbiol* 2011;**77**:1405–12.

McMillan JD, Wang DIC. Mechanisms of oxygen transfer enhancement during submerged cultivation in perfluorochemical-in-water dispersionsa. *Ann NY Acad Sci* 1990;**589**:283–300.

Melton ED, Swanner ED, Behrens S *et al*. The interplay of microbially mediated and abiotic reactions in the biogeochemical Fe cycle. *Nat Rev Micro* 2014;**12**:797–808.

Nelson D, Jannasch H. Chemoautotrophic growth of a marine Beggiatoa in sulfide-gradient cultures. *Arch Microbiol* 1983;**136**:262–9.

Neubauer SC, Emerson D, Megonigal JP. Life at the energetic edge: kinetics of circumneutral iron oxidation by lithotrophic iron-oxidizing bacteria isolated from the wetland-plant rhizosphere. *Appl Environ Microbiol* 2002;**68**:3988–95.

Park B, Dempsey BA. Heterogeneous oxidation of Fe(II) on ferric oxide at neutral pH and a low partial pressure of O_2. *Environ Sci Technol* 2005;**39**:6494–500.

Pfennig N. *Rhodocyclus purpureus* gen. nov. and sp. nov., a ring-shaped, vitamin B12-requiring member of the family Rhodospirillaceae. *Int J Syst Evol Microbiol* 1978;**28**:283–8.

Rentz JA, Kraiya C, Luther GW *et al*. Control of ferrous iron oxidation within circumneutral microbial iron mats by cellular activity and autocatalysis. *Environ Sci Technol* 2007;**41**:6084–9.

Revsbech NP. An oxygen microsensor with a guard cathode. *Limnol Oceanogr* 1989;**34**:474–8.

Rickard D, Luther GW. Chemistry of iron sulfides. *Chem Rev* 2007;**107**:514–62.

Roden E, Sobolev D, Glazer B *et al*. Potential for microscale bacterial Fe redox cycling at the aerobic-anaerobic interface. *Geomicrobiol J* 2004;**21**:379–91.

Singer PC, Stumm W. Acidic mine drainage: the rate-determining step. *Science* 1970;**167**:1121–3.

Slowey A, Marvin-DiPasquale M. How to overcome interelectrode variability and instability to quantify dissolved oxygen, Fe(II), mn(II), and S(II) in undisturbed soils and sediments using voltammetry. *Geochem Trans* 2012;**13**:6.

Sobolev D, Roden EE. Suboxic deposition of ferric iron by bacteria in opposing gradients of Fe(II) and oxygen at circumneutral pH. *Appl Environ Microbiol* 2001;**67**:1328–34.

Straub KL, Benz M, Schink B *et al*. Anaerobic, nitrate-dependent microbial oxidation of ferrous iron. *Appl Environ Microbiol* 1996;**62**:1458–60.

Stumm W, Sulzberger B. The cycling of iron in natural environments: considerations based on laboratory studies of heterogeneous redox processes. *Geochim Cosmochim Acta* 1992;**56**:3233–57.

Stumm W, Morgan JJ. *Aquatic Chemistry: Chemical Equilibria and Rates in Natural Waters*. New York: Wiley, 1996.

Sun W, Nešić S, Woollam RC. The effect of temperature and ionic strength on iron carbonate ($FeCO_3$) solubility limit. *Corros Sci* 2009;**51**:1273–6.

Sung W, Morgan JJ. Kinetics and product of ferrous iron oxygenation in aqueous systems. *Environ Sci Technol* 1980;**14**:561–8.

Swanner ED, Nell RM, Templeton AS. Ralstonia species mediate Fe-oxidation in circumneutral, metal-rich subsurface fluids of Henderson mine, CO. *Chem Geol* 2011;**284**:339–50.

Taillefert M, Bono AB, Luther GW. Reactivity of freshly formed Fe(III) in synthetic solutions and (pore)waters: voltammetric evidence of an aging process. *Environ Sci Technol* 2000;**34**:2169–77.

Tamura H, Goto K, Nagayama M. The effect of ferric hydroxide on the oxygenation of ferrous ions in neutral solutions. *Corros Sci* 1976;**16**:197–207.

Tamura H, Kawamura S, Hagayama M. Acceleration of the oxidation of Fe^{2+} ions by Fe(III)-oxyhydroxides. *Corros Sci* 1980;**20**:963–71.

Taylor SR. Abundance of chemical elements in the continental crust: a new table. *Geochim Cosmochim Acta* 1964;**28**:1273–85.

Tschech A, Pfennig N. Growth yield increase linked to caffeate reduction in *Acetobacterium woodii*. *Arch Microbiol* 1984;**137**:163–7.

Weber KA, Achenbach LA, Coates JD. Microorganisms pumping iron: anaerobic microbial iron oxidation and reduction. *Nat Rev Micro* 2006;**4**:752–64.

Weiss J, Emerson D, Backer S *et al*. Enumeration of Fe(II)-oxidizing and Fe(III)-reducing bacteria in the root zone of wetland plants: implications for a rhizosphere iron cycle. *Biogeochemistry* 2003;**64**:77–96.

Weiss JV, Rentz JA, Plaia T *et al*. Characterization of neutrophilic Fe(II)-oxidizing bacteria isolated from the rhizosphere of wetland plants and description of *Ferritrophicum radicicola* gen. nov. sp. nov., and *Sideroxydans paludicola* sp. nov. *Geomicrobiol J* 2007;**24**:559–70.

Widdel F, Schnell S, Heising S *et al*. Ferrous iron oxidation by anoxygenic phototrophic bacteria. *Nature* 1993;**362**:834–6.